ORIGINAL PAPER

A study on the prediction of displacement in the accelerated deformation stage of the creep bedding rock landslides

Zechuang Li[1] · Peifeng Cheng[1]

Abstract

In view of the complexity, randomness, and uncertainty of landslide evolution, it causes substantial damage to the environment every year, in the absence of a mature model for landslide displacement prediction. Most of bedding landslides are characterized by creep, and its displacement in the accelerated deformation stage changes with time in line with the law extremely similar to that of rock creep. From the perspective of the rock creep theory, a nonlinear viscous component is proposed, and a model for predicting the displacement in the accelerated deformation stage regarding creep landslides is established by combining it with the plastic component. The cumulative displacement-time series data at the monitoring points is input as the parameters, and the model parameters are obtained via the nonlinear fitting of the model parameters, and thereafter the prediction of landslide displacement in the accelerated deformation stage is rendered possible. Taking the landslide on the South Slope of West Open-pit Mine in Fushun and the Jimingsi landslide as the research cases, the newly proposed displacement prediction model is employed to analyze and predict the cumulative displacement of landslides. By comparing the measured and predicted values at the selected prediction time points in the initial stage of accelerated deformation and in the pre-sliding stage, it is found that, in these two landslides, the maximum relative error (RE) at each monitoring point and each prediction time point in the initial stage and the pre-sliding stage of accelerated deformation is respectively less than 2% and less than 7%, and that the correlation coefficient of predicted and measured values of displacement in the phase of accelerated deformation is greater than 0.99, and the results show that the proposed model for predicting the displacement of creep bedding rock landslides has satisfactory accuracy and applicability, and can meet the demand of landslide displacement prediction and serve as an effective way to prevent the environmental risk posed by landslides.

Keywords Landslide · Creep · Accelerated deformation stage · Displacement prediction · Nonlinear viscous component

Introduction

Bedding rock slopes are often encountered in the construction of railway, highway, open-pit mining, and water conservancy, and environmental damages and severe accidents caused by such slopes take place regularly. In 1963, a huge bedding rock landslide occurred on the left bank of Vaiont Reservoir in Italy and led to a major accident in which the landslide size was approximately 200 to 300 million m^3 and more than 3000 people died; the Chengkun Railway West landslide was a bedding rock landslide too, with a thickness of 14 m, a volume of 2.2 million m^3, which buried the railway for a length of 160 m and disrupted traffic for 40 days, causing serious economic losses. According to the forecasts from meteorological and seismic departments, at the beginning of this century, climate change and earthquakes tend to be active, extreme weather events will be on the rise, and seismic activity is of high frequency, so that the natural factors inducing landslides are active in the long term, resulting in high-frequency trend of landslides.

In recent years, many scholars have done a lot of research on the instability of bedding rock slopes (Lo et al., 1978; Xu et al., 2013; Hamouda & El-Gharabawy, 2019; Li & Cai, 2020). These slopes are divided into two categories: those simple dip slopes with a potential sliding surface inclination less than the

---

✉ Peifeng Cheng
  chengpeifeng@nefu.edu.cn

  Zechuang Li
  lzc@nefu.edu.cn

[1] School of Civil Engineering, Northeast Forestry University, Harbin 150040, Heilongjiang, China

slope angle, usually characterized by a "creep-sliding-fracturing" slide of the bedding (Huang, 2007), and the others are dip slopes which have a potential sliding surface inclination greater than the slope angle, whose geological-physical model under the control of the weak interlayer between the slope layers usually presents itself as the "sliding-bending-fracturing" mode (Huang, 2007), and such a slope can be divided into two parts of different deformation properties, that is, the upper middle section with the bedding plane slip and the lower bend-rise section. By analyzing the deformation characteristics of these two types of bedding rock landslides, it is found that the dip layered slopes, when evolving from deformation to instability, go through a long process of temporal deformation, and the deformation of the bedding landslides mostly features the creep, and their deformation process conforms to the law extremely similar to that of the creep of soil and rock slopes, namely its deformation (cumulative displacement) - time curve features three stages of evolution temporally: the initial deformation stage, the even-speed deformation stage, and the accelerated deformation stage (which can be subdivided into the initial stage of accelerated deformation and the pre-sliding stage). For the creep bedding rock landslides, before a landslide occurs, it is bound to go through the stage of accelerated deformation. Therefore, the analysis of the law regarding the trend of accelerated growth of landslide deformation should be given great attention.

In the studies on landslide prediction, many scholars at home and abroad have carried out a lot of research on the prediction of displacement by examining the landslide displacement data. Saito (Saito, 1965) analyzed and depicted the process of deformation and destruction of soil under various pressures, and for the first time put forward the classical three-stage theory of soil creep and destruction, and established the Saito model. Kennedy (Kennedy, 1971) used the method of curve fitting about landslide displacement to predict the time of landslide-incurred damages, and achieved remarkable research results. Brown and Hoek (Brown & Hoek, 1978) proposed the extension of the landslide deformation monitoring curve based on monitoring data from the slope of the Chichcamata mine in Chile. Li et al. (Li et al., 2009) employed the wavelet analysis and mutation method to perform a prediction study on landslide displacement. Xu et al. (Xu et al., 2011) used the method of moving average to break down the cumulative displacement of landslides, and used the GM (1, 1) gray model and the self-regression AR model respectively to predict the displacement of landslides in trend and period. Xue et al. (Xue et al., 2014) proposed a new prediction and forecasting method with the displacement data of the accelerated deformation as the input parameters, and the applicability of the new method is verified by the Vaiont landslide and the Xintan landslide. Zhou et al. (Zhou et al., 2016) used the timing analysis and PSO-SVM model to predict the displacement of the Bazimen landslide in the Three

Gorges Reservoir. Miao et al. (Miao et al., 2018) and Li et al. (Li et al., 2019a) used SVR model and multi-algorithm parameter optimization method for prediction and research about stepwise landslides. At present, a variety of existing mathematical models are not yet mature and have not really been tested by engineering practice; landslide displacement prediction mainly depends on the mathematical inference of displacement monitoring curve, whereas the actual process of landslide evolution and its internal laws cannot be fully revealed (Wang et al., 2008), both of which need to be continuously improved and perfected in practice, and the practical application of theoretical research results is still in the phase of in-depth research.

The law governing the displacement of creep bedding rock landslides is in line with the three stages of rock creep, and the essence of the deformation and destruction of the landslide mass is the realization of the rock creep theory. Because of the problem of poor applicability and practicality of the current theoretical model for landslide prediction, the creep of rock as its prominent nature plays a crucial role in the prediction of the displacement of landslides in the accelerated deformation stage. This paper starts with the analysis of the creep nature of rock, and by studying the strain-time relationship in the stage of accelerated creep of rock; based on the theory of rock creep, a nonlinear viscous component is proposed, so that a suitable creep model is proposed through the combination with plastic components and a model for predicting the displacement of bedding rock landslides in the accelerated deformation stage is established. By solving the nonlinear fitting of the model parameters, the model parameters are obtained and then the development trend of landslide displacement is predicted. Taking the landslide on the South Slope of West Open-pit Mine (hereafter referred to as SSWOPP landslide) ("sliding-bending-fracturing" type) and Jimingsi landslide ("creep-sliding-fracturing" type) as the research cases, the displacement prediction of these two landslides is carried out using this model. Compared with the actual deformation of the landslides, it is verified that the newly proposed prediction model can accurately reflect the deformation characteristics and trend of the bedding rock landslide, and the prediction of the landslide displacement is of great significance to environmental protection (Zhang et al., 2019a; Luo et al., 2020; Dong et al., 2018; An & Sun, 2020).

The proposition of the predictive model for the displacement of creep bedding rock landslides

In creep mechanics, the basic creep component models include perfectly elastic solids (Hooke), ideally viscous liquids (Newtons), and perfectly plastic bodies (St. Venant). The traditional component model is a linear combination of model

components, and because the viscosity coefficient η of Newtonian body is a constant, the final model can only reflect the linear-elastoplasticity characteristics and cannot represent the accelerated creep stage (no matter how many components there are in the model or how complex the model is), for the traditional creep model regards rock as the ideal Newtonian body. In fact, the creep of rock also has non-Newtonian properties (Kang & Zhang, 2014).

According to the theory of rock creep, the deformation and damages of landslides are the result of internal stress and the strength of rock which change over time, and the displacement is a direct reflection of this change. The law governing the displacement of landslides conforms to the three stages of rock creep, and the essence of landslide deformation and destruction is the realization of rock creep theory. Therefore, the creep of rock plays an important role in the prediction of landslide displacement, and it is of necessity to study the law unveiling how displacement changes over time during landslide deformation on the basis of the theory of rock creep, and to establish a predictive model for landslide displacement in the accelerated deformation stage.

New nonlinear viscous components

The creep of rock is a very complex problem, so creep-related models are often used to visualize its complexity. As rock enters the accelerated creep stage, and with the cracks in the rock continuing to expand, the creep velocity increases nonlinearly with time and the viscosity coefficient decreases over time. Based on the mechanic properties of rock in the accelerated creep stage, a new nonlinear viscous component is proposed and the viscosity coefficient η is the non-stationary parameter η(t) related to time.

$$\eta(t) = \eta_0 e^{-nt} \tag{1}$$

In Eq. (1), η_0 is the initial viscosity coefficient and n is the creep index reflecting the rock's degree of change of the accelerated creep velocity. When $n = 0$, the nonlinear viscous body becomes a Newtonian body.

The constitutive equation of the model components is:

$$\tau = \eta(t)\dot{\gamma} = \eta_0 t^{-nt}\dot{\gamma} \tag{2}$$

In Eq. (2), τ is the shearing stress while $\dot{\gamma}$ the shearing strain rate.

When $t = 0$, $\gamma(0) = \dot{\gamma}(0) = 0$, Laplace transform is performed on it, then:

$$\widetilde{\gamma} = \frac{\tau}{\eta s(s-n)} \tag{3}$$

In Eq. (3), $\widetilde{\gamma}$ is the Laplace transform of γ and s is the complex variable of the Laplace transform. Carrying out

inverse Laplace transform on it, the creep equation of the nonlinear viscous body can be obtained:

$$\gamma = \frac{\tau}{n\eta}(e^{nt}-1) \tag{4}$$

Proposal of predictive model for landslides

The nonlinear viscous body and the plastic body are connected in parallel to (referred to as "||" sign) form a nonlinear viscoplastic body that can reflect the characteristics of rock's accelerated creep, as shown in Fig. 1.

The corresponding creep equation is:

$$\gamma = \frac{H(\tau_0-\tau_\infty)}{n\eta}(e^{nt}-1) \tag{5}$$

In Eq. (5), τ_0 is the constant shearing stress, τ_∞ is the long-term strength against shearing, and H can be expressed by the following formula:

$$H(\tau_0-\tau_\infty) = \begin{cases} 0 & (\tau_0 \leq \tau_\infty) \\ \tau_0-\tau_\infty & (\tau_0 > \tau_\infty) \end{cases} \tag{6}$$

When the stress level τ_0 is greater than a certain value τ_∞, the growth of strain with time does not converge to a certain value, but an accelerated creep stage appears, which has plastic characteristics. The new rock creep model proposed breaks through the traditional concept of ideally Newtonian medium and can better describe the characteristics of rock creep.

In light of the abovementioned nonlinear creep model for rock, and targeting the landslide displacement prediction in the accelerated deformation stage, it is viable to reset the deformation at the beginning of the accelerated deformation stage to zero, and set the accumulated time series monitoring data in the accelerated deformation stage as the required parameters for prediction. This paper proposes a new predictive model for creep bedding rock landslide displacement during the accelerated deformation stage. The expression of this model is:

$$S = \frac{\tau_0-\tau_\infty}{n\eta}(e^{nt}-1) \tag{7}$$

In Eq. (7), S is the landslide displacement value, τ_0 is the constant shearing stress, τ_∞ is the long-term strength against
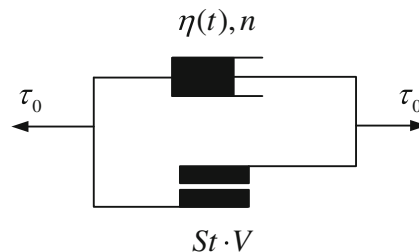

Fig. 1 Schematic diagram of Nonlinear Newton‖St. Venant creep model

shearing, η is the viscosity coefficient, n is the creep index, and t is the monitoring time. The nonlinear fitting method is applied to fit the displacement-time data $(t_i, S_i)(i = 1,2,\ldots,n)$, and the coefficients $\frac{\tau_0 - \tau_\infty}{\eta_0}$ and n of the prediction model are obtained.

This predictive model for landslide displacement offers a prediction with dynamic tracking. During the prediction, every time a new piece of observation data is obtained, the landslide parameters are processed and substituted into the predictive model for prediction, and each monitoring point can get a definite solution, namely to use the latest changing characteristics of the landslide to make predictions, so as to achieve real-time tracking and prediction.

Model evaluation

In this paper, the effect of fitting the model-predicted data to the measured data is used as one of the standards for comparing model prediction accuracy, and correlation coefficient R (Saccenti et al., 2020), relative error (RE) (Wang et al., 2018), and the average relative error (ARE) (Huang et al., 2020) are used to quantify the performance of the predictive model for displacement.

$$R = \sqrt{\frac{\left[\sum\limits_{i=1}^{m}\left(S - \overline{S}\right)\sum\limits_{i=1}^{m}\left(S_i - \overline{S_i}\right)\right]^2}{\sum\limits_{i=1}^{m}\left(S - \overline{S}\right)^2\sum\limits_{i=1}^{m}\left(S_i - \overline{S_i}\right)^2}} \tag{8}$$

$$RE = \frac{|S_i - S|}{S_i} \tag{9}$$

$$ARE = \frac{1}{m}\sum_{i=0}^{m}\frac{|S_i - S|}{S_i} \tag{10}$$

where S_i is the measured value, $\overline{S_i}$ is the average measured value, S is the predicted value, overlined S is the average predicted value, and m is the measured node number. The values of R, RE, and ARE range from 0 to 1. R assesses the fit between the predicted values and the measured values; the higher the value of R, the better the fit between the measured and predicted values. Additionally, RE indicates the estimation error and ARE indicates the average estimation error during the entire monitoring period. The smaller the values of RE and ARE, the smaller the prediction errors.

Cases of creep bedding rock landslides

The SSWOPP landslide

The SSWOPP landslide engineering geological overview

The SSWOPP landslide is located in the west of Fushun City, Liaoning Province, China. It is a typical bedding rock landslide ("sliding-bending-fracturing" type). Since the landslide

was discovered in 2010, scholars have carried out a lot of research on the landslide. Nie et al. (Nie et al., 2015) analyzed the deformation characteristics and mechanism of the landslide based on the original data of site survey and investigation. Nie et al. (Nie et al., 2017) proposed a landslide failure prediction mathematical model to predict the failure time of landslide static GPS monitoring points. Zhang et al. (Zhang et al., 2019b) utilized geological radar DInSAR, microseismic technology, and numerical simulation methods to determine the location of the landslide boundary and stability of the landslide (Huang & Zheng, 2019; Qin et al., 2019; Li et al., 2019b). Based on the above research results, this paper focuses on analyzing and verifying the applicability and accuracy in displacement law prediction of the newly proposed displacement prediction model in the acceleration deformation stage of the bedding rock ("sliding-bending-fracturing" type) landslide.

The SSWOPP landslide is almost elliptical in plane, the head edge (south side) is wide, the foot edge (north side) is slightly narrowed, the width is about 1.5 km in the north-south direction, and the longitudinal length in the east-west direction is about 3.1 km. The depth of the sliding surface is more than 100 m, with a total volume of about 300 million m^3, and it is a super large deep rock landslide. The ground fissures at the crown of the SSWOPP landslide control the southern boundary of the landslide, and the F_5 and F_{3-1} faults control the east and west boundary positions of the landslide body in the pit, as shown in Fig. 2 (Beijing 54 coordinate system, referred to as BJ54).

Through the survey of the SSWOPP landslide, it was found that the rock formations and the slopes were inclined to the north, and the dip angle of the two was basically the same, which was a consequent layered structure. The weak discontinuities in basalt rock mass and the unconformity interface between granite gneiss and basalt constitute a potential sliding surface. The dip angle (about 30°) of the potential sliding surface is greater than the slope angle (19°–27°). The deformation and failure mode of the SSWOPP landslide is a sliding-bending-fracturing type (Nie et al., 2015).

During the survey, the RG downhole television camera produced by the British RG (Robertson Geologging Ltd) was used in the downhole hammer borehole to perform in-well video recording. This system used the principle of imaging the borehole wall. Through the analysis of the rock formation, a complete image of the borehole wall can be presented. The monitoring image of the borehole can be analyzed by software, and data such as the well log, the expanded view of the borehole wall, and the dip angle of the joints and fracture zone can be obtained. Each borehole wall image starts from North (N) direction and expands in the order of North (N)→ East (E)→S (South)→West (W)→N (North) direction. Taking the qkcw41 borehole as an example, the image of the TV data processing at the depth of the hole from 93–98
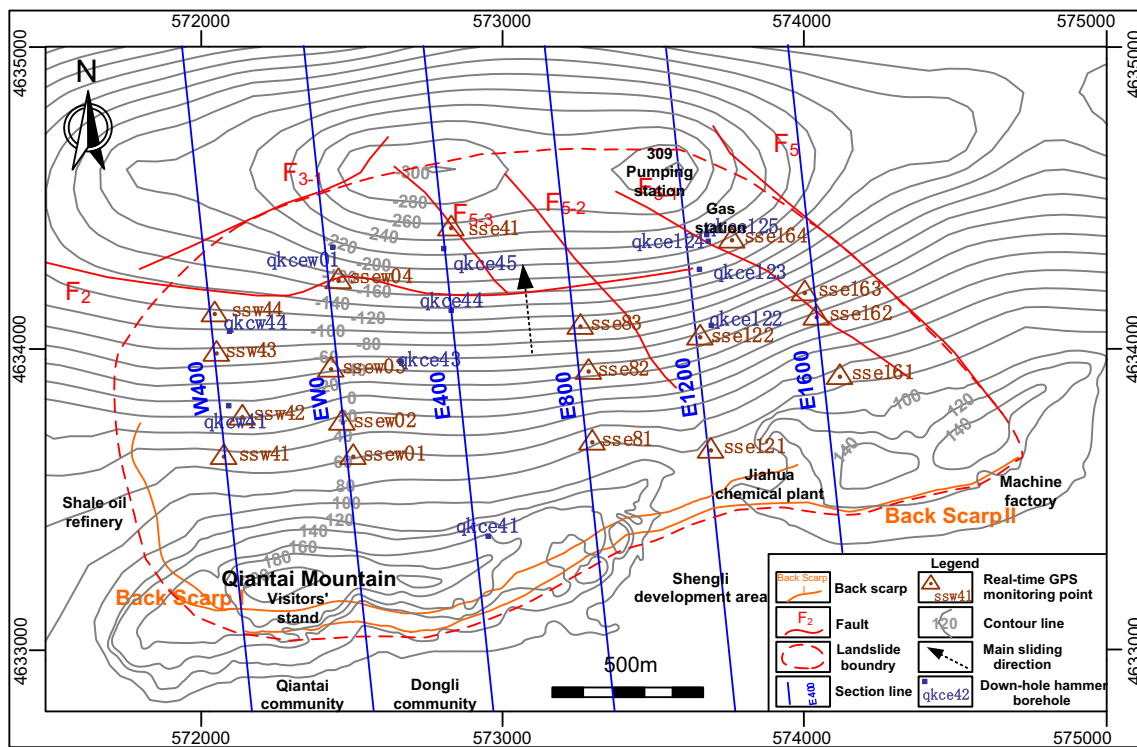
Fig. 2 Topographical map of the landslide, with the distribution of GPS monitoring points and downhole hammer borehole

m is shown in Fig. 3. The number on the left is the depth of the borehole, and the image of the borehole wall starts with N (0°), and then N→E→S→W→N is unfolded at 360°, the middle image shows the dip angle of the joints and fracture zone, and the two pictures on the right show the occurrence of joints and fracture zone at 315° and 45°.

Eleven video boreholes in the well were arranged with a cumulative video depth of 1507.3 m. The geological data of downhole hammer drilling were supplemented and improved to some extent, which made up for the shortcomings of downhole hammer drilling. The borehole video observation information is shown in Table 1.

Through the analysis of the video results in the well, it can be seen that the rock mass joints of the landslide are relatively developed, and the middle and lower landslides are cut by faults F_2, F_{5-1}, F_{5-2}, and F_{5-3}. And the rock mass structure is fragmentary in part, generally, which belongs to the soft-hard layered structure slope controlled by multiple weak layers.

The SSWOPP landslide monitoring data analysis

On April 13, 2013, 5 real-time GPS monitoring points were deployed on the landslide body (see Fig. 2), which were located on the E400, E800, and E1200 monitoring profiles, namely sse41, sse81, sse82, sse121, and sse122. The monitoring was performed once a day. The horizontal velocity and vertical velocity-time process curves of the real-time monitoring points of sse41, sse81, sse82, sse121, and sse122 are

shown in Fig. 4 (the vertical displacement is positive for upward and negative for downward).

According to the velocity-time curve characteristics of real-time GPS monitoring points and investigation results, the deformation evolution process of landslide is divided into two stages: initial deformation and constant velocity deformation (August 2010 to March 17, 2013), and accelerated deformation stage (March 18, 2013, to March 9, 2014). The accelerated deformation stage can also be subdivided into the initial stage of accelerated deformation (March 18, 2013, to January 12, 2014) and the pre-sliding stage (January 13, 2014, to March 9, 2014).

The SSWOPP landslide displacement prediction

The starting date of real-time GPS monitoring points sse41, sse81, sse82, sse121, and sse122 was April 13, 2013, which monitored the whole process of the accelerated deformation stage of the landslide. These GPS monitoring points were distributed in different positions of the landslide, which could better reflect the displacement characteristics and development trend of the landslide. These monitoring points can be used for the displacement prediction of the SSWOPP landslide. The accelerated stages of July 16, 2013, and January 22, 2014, were selected as the representative prediction time points, and the time series displacement value from the starting time of the accelerated deformation stage (the corresponding initial displacement value is $S_0 = 0$) to the day before

Fig. 3 The image of the qkcw41 borehole TV data processing
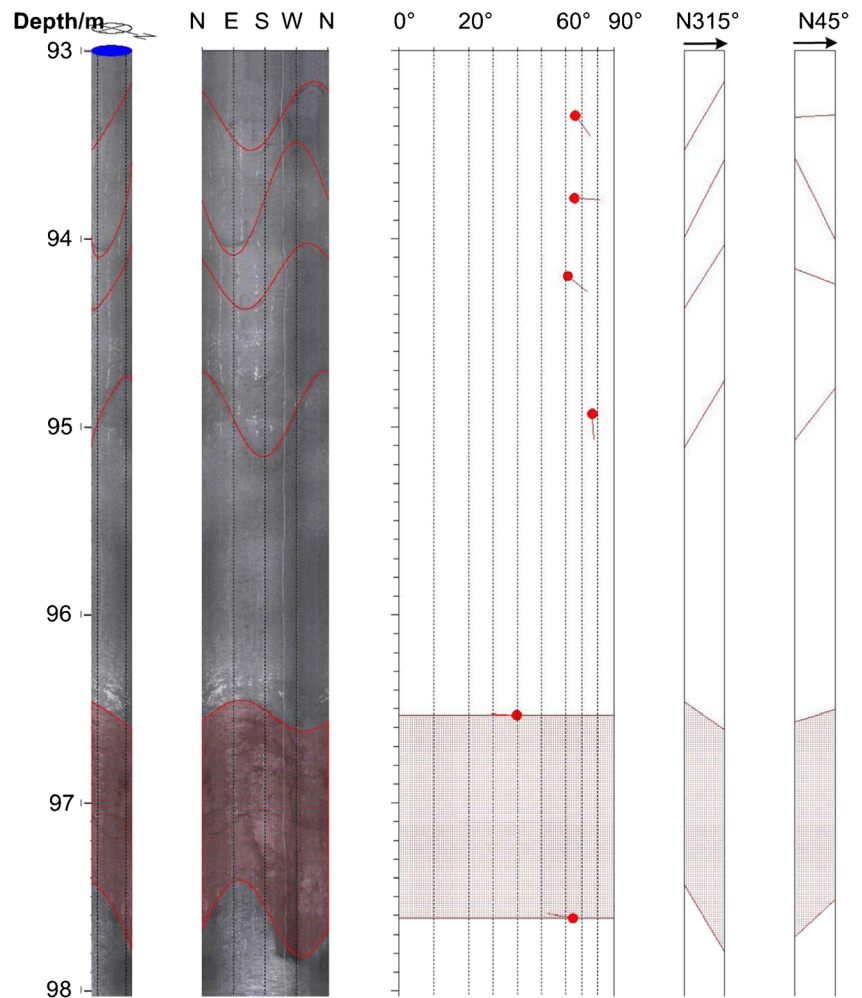
the prediction time point (S_{t-1}) was selected as the input data to predict the displacement value S at the time point and compared it with the actual value S_t at the predicted point; that is, the monitoring data from April 13, 2013, to July 15, 2013, were selected to predict the cumulative displacement value on July 16, 2013, in the initial stage of accelerated deformation; and the monitoring data from April 13, 2013, to January 21, 2014, were selected to predict the cumulative displacement value on January 22, 2014, during the pre-sliding stage.

It can be seen from the data in Table 2 that the average value of RE between the measured displacement values and the predicted values of the five monitoring points on July 16, 2013, in the initial stage of accelerated deformation is 1.49%, while the predicted displacement value of the pre-sliding stage on January 22, 2014, was also very close to the measured value, and the average value of RE is 6.05%, indicating that the model can reflect the trend of landslide displacement.

From the analysis results of the above two-part displacement time series data in Table 3, the R between the predicted displacement value and the measured value during the period of Apr. 13, 2013–Jul. 16, 2013, is greater than that of the

period of Apr. 13, 2013–Jan. 22, 2014, and the ARE is less than that of the period of Jan. 22, 2014, which shows that the prediction accuracy of this model in the initial stage of accelerated deformation is higher than that of the pre-sliding stage, and which also reflects that the higher the accuracy within the short term, the greater the error there will be with time.

The Jimingsi landslide

The Jimingsi landslide engineering geological overview

The Jimingsi landslide is located in Zigui County, Yichang City, Hubei Province, and the landslide occurred in the clay rocks and shale of sandstone sandwiched with carbonaceous substance in the Triassic and Jurassic systems, which is a bedding landslide at the shallow layer of bedrock ("creep-sliding and fracturing" type) (Liu et al., 2014; Wang et al., 2014; Lv, 1994; He et al., 2016). The entire landslide area extends for a length of 250–300 m; the maximum width measures about 150 m; the average thickness of the mass is 15 m; the total volume is about 600,000 m^3; it can be classified into

Table 1 Borehole information of video observation in well

Section line	Borehole number	Borehole top elevation (m)	Drilling depth (m)	Observational depth (m)	Distance between main fractured part and borehole top
W400	qkcw41	− 21.62	240	122	91.29~96.13
	qkcw44	− 78.69	105	89	114.44~116.01
EW0	qkcew01	− 172.92	153	73	71.46~74.95
E400	qkce41	147.06	75	75.5	-
	qkce43	− 53.87	279	230	52.91~58.06
					119.3~121.7
					145.39~147.15
					175.9~177.52
	qkce44	− 131.67	201	160.8	47~47.5
					84.9~108.5
					120.5~160.8
	qkce45	− 202.45	141	143.5	49~51.7
					73~78
					108~109
					116.4~117.6
					122.75~125.61
E1200	qkce122	− 72.96	282	223	156.8~166.0
					192.5~199.1
	qkce123	− 156.46	150	143.5	39.6~50.5
					139.5~143.3
	qkce124	− 188.48	117	112.7	103~108
	qkce125	− 182.46	186	134.3	25~26
					41.6~42.3
					130.2~132.6

small and medium-sized landslides, of which the map (Lv, 1994) is shown in Fig. 5.

The rock formation system of the landslide consists of thick layers of blocky ash rock in the Triassic system, which is sandwiched with marlstone and calcium shale. To the west of the landslide are clay rock in the middle series of the Triassic system, and the carbonaceous shale in the upper series of the Triassic system and in the lower series of the Jurassic system. The structure is loose, and the strength against shearing is relatively low. The bedrock is covered with eluvial layers of uneven thicknesses ranging from 0 to 10 m in the Quaternary system. The elevation of the front edge of the landslide is about 250 m, and that of the rear edge is nearly 480 m. The strata tendency and slope tendency are generally the same, belonging to the downhill slope, and the terrain is high in the east and low in the west. The northern edge of the landslide lies a quarry at the cement plant of Zigui County, with a mining width of 153 m and the free surface of the

Fig. 4 Velocity-time curve of real-time GPS monitoring points between Apr. 13, 2013, and Apr. 30, 2014. **a** Horizontal velocity-time curve. **b** Vertical velocity-time curve
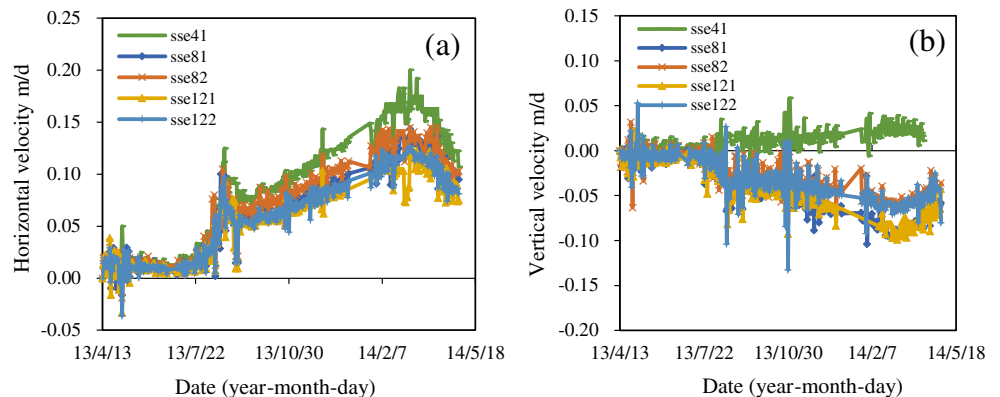
Table 2 Comparison of predicted and actual values of cumulative displacements of the SSWOPP landslide

Monitoring points	Jul 16, 2013			Jan 22, 2014		
	Predicted value S (cm)	Measured value S_t (cm)	Relative error RE (%)	Predicted value S (cm)	Measured value S_t (cm)	Relative error RE (%)
sse41	132.74	134.59	1.37	1991.70	1892.12	5.26
sse81	125.77	127.79	1.57	1811.02	1709.15	5.96
sse82	122.56	124.32	1.42	1803.58	1702.95	5.91
sse121	117.21	119.20	1.67	1671.24	1565.14	6.78
sse122	104.46	105.96	1.41	1578.17	1484.32	6.32

quarry area measuring 70 to 80 m in height. The north and south sides of the landslide both have gullies that run basically in the east-west direction, laying the structural foundation for the formation of the landslide.

There develop fractures in this area, with relatively concentrated pressures. In the head of the landslide mass, there is a faulted fracture zone running in the north-northeast direction, north-northwest inclining, whose inclination is 65°, and which measures about 5 m in width, affecting an area as wide as tens of meters. It is composed of loose mylonite and breccia, with weak cementation, and is the control structure of the arc of the head of the landslide. There are two groups of joints in the bedrock of the landslide mass: one group goes in the north-west direction at 30°, inclining to south-west at 65°, and the other group goes north-east at 20°–30°, inclining to south-east at 55°. The fractures and the joints interact and cut the bedrock into masses of different sizes, thus laying a structural foundation for the formation of landslides.

### The Jimingsi landslide monitoring data analysis

The Jimingsi landslide took 1 year and 3 months from its discovery to its main slide. Through the macro-analysis of the geological features, hydrological and surface deformation of the landslide of Jimingsi, it is found that the Jimingsi landslide has gone through 3 stages of development: (1) initial deformation (1990.03.05–1991.02.03): cracks were found

above the quarry of the cement plant in Zigui County on March 5, 1990. Ten simple observation points were set up on the north and south back cracks in consideration of the stability of the outer bedrock of the cracks on April 24, 1990 (Fig. 5). Each observation point consists of a fixed point and a mobile point: the former is fixed on a stable bedrock or soil layer on the outside of the crack, while the mobile point is located in the deformed body. The observation points like G_5, G_6, G_7, G_8, G_9, and G_{10} in the figure are located on the cracks at the head of the deformation body, and the line connecting their own fixed point and mobile point is arranged perpendicular to the direction of the cracks; G_1 and G_4 are located on the cracks at the edge of the deformation body, which is for the purpose of measuring the initial displacement of the measured points and the direction of the main slickenside on the crack parallel with the line connecting the points. Each observation point mainly uses a steel ruler to measure the oblique distance between the fixed and mobile points, and meanwhile to observe and record the changes of crack tension and fault height; with the arrival of the rainy season of 1990, the tensile cracks gradually enlarged in both width and length, and a few tensile cracks passed through, the faults enlarged, and the creep and deformation were obvious. (2) Even-speed deformation (1991.02.04–1991.04.30): in March 1991, the sliding surface of the landslide began to pass through, the new small fissures at the head of the landslide increased, and the main cracks were no longer distributed intermittently but gradually passed

Table 3 Comparison of cumulative predicted displacement value and actual displacement value of the SSWOPP landslide

Monitoring points	Apr 13, 2013–Jul 16, 2013				Apr 13, 2013–Jan 22, 2014			
	Model parameters		R	ARE (%)	Model parameters		R	ARE (%)
	$(\tau_0 - \tau_\infty)/\eta_0$	n (10^{-2})			$(\tau_0 - \tau_\infty)/\eta_0$	n (10^{-2})		
sse41	1.601	− 0.293	0.999	3.87	1.399	0.933	0.997	17.18
sse81	1.634	− 0.460	0.999	2.42	1.288	0.927	0.997	15.49
sse82	1.557	− 0.409	0.999	2.16	1.277	0.929	0.997	15.94
sse121	1.462	− 0.368	0.999	3.85	1.210	0.921	0.996	16.07
sse122	1.225	− 0.232	0.998	4.28	1.109	0.933	0.996	17.38

Fig. 5 The map of Jimingsi landslide (Lv, 1994)

Fig. 6 The geological profile of the Jimingsi landslide
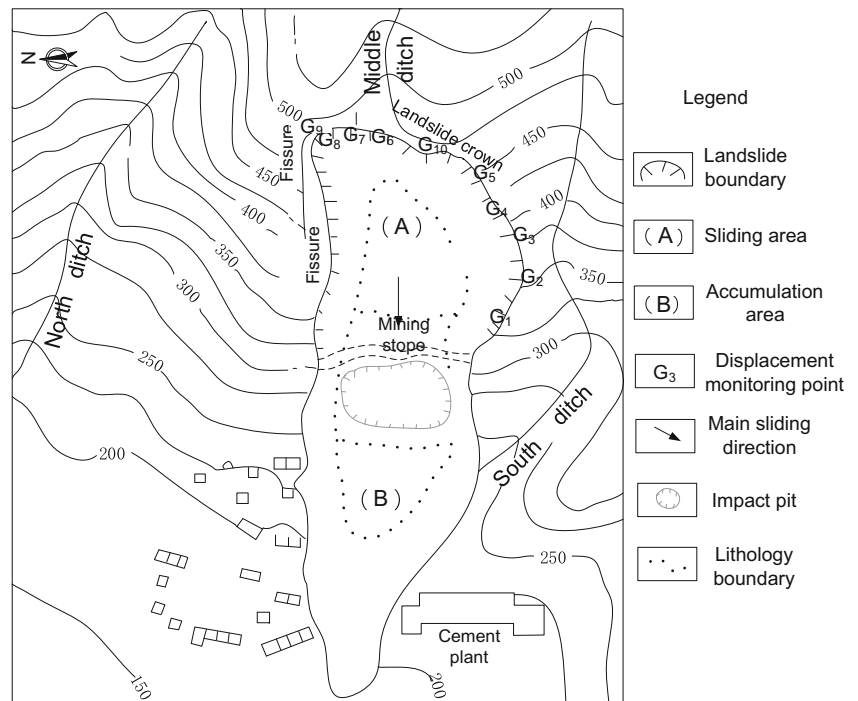
through; there was no appreciable associated phenomenon. (3) Accelerated deformation (1990.05.01–1991.06.29): after May 1990, the amount of deformation of the landslide gradually increased, the rate of deformation quickened, the new small cracks on the surface of the landslide increased, the size of cracking enlarged, and the main crack obviously connected into an arc shape; after June 26, 1991, the deformation of the landslide entered the pre-sliding phase, and in the early hours of June 29, 1991, the main landslide body slid at once, with a volume of about 600,000 m^3. The landslide debris was tongue-shaped in a ditch on the west side of the cement plant, covering an area of about 70,000 m^2, and its geological profile (Lv, 1994; He et al., 2016) is shown in Fig. 6.

The Jimingsi landslide displacement prediction

The monitoring areas, including G_1, G_4, G_6, G_7, and G_8, are the key areas of landslide instability, and hence the monitoring points G_1, G_4, G_6, G_7, and G_8, which can represent the deformation traits of the landslide, are selected to predict the displacement in the initial stage of accelerated deformation and in the pre-sliding stage. Having considered the stages used to depict the deformation of landslides, May 31, 1991, and June 26, 1991, which are within the period of accelerated deformation, are selected as the representative point of time for prediction, and the timing displacement values from the starting point of the accelerated deformation to the day before the point of time for prediction as the input data to forecast the displacement at the selected points of time.

It can be seen from the data in Table 4 that the average value of RE between the measured and predicted values of displacement at the five monitoring points on May 31, 1991, in the initial stage of accelerated deformation is 0.908%, while the predicted and measured values of displacement on June 26, 1991, in the pre-sliding stage are also very close, and the average value of RE is 5.83%, indicating that the model displays a good performance in prediction and can reflect the displacement trend of landslides.

Judging from the results of the analysis regarding the two segments of timing data in relation to displacement (Table 5), the R of the predicted and measured values of displacement during the period from 1991.5.1 to 1991.5.31 is greater than that from 1991.5.1 to 1991.6.26, and the ARE within the former period is smaller than that within the latter period,
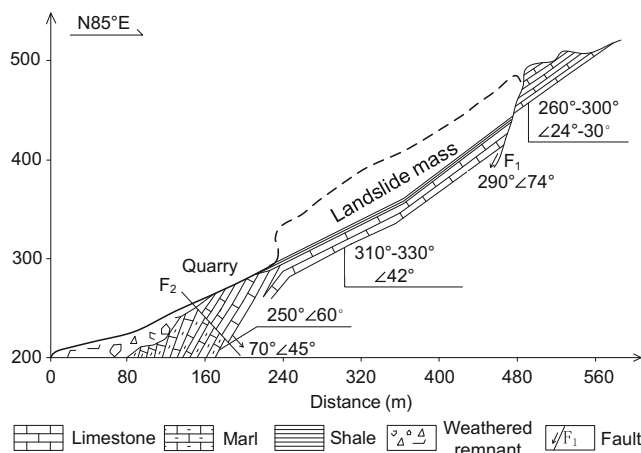
Table 4 Comparison of predicted and actual values of cumulative displacements of the Jimingsi landslide

Monitoring points	May 31, 1991			Jun 26, 1991		
	Predicted value S (cm)	Measured value S_t (cm)	Relative error RE (%)	Predicted value S (cm)	Measured value S_t (cm)	Relative error RE (%)
G_1	20.10	20.37	1.32	105.11	100.19	4.91
G_4	34.58	34.81	0.65	112.52	120.11	6.31
G_6	22.89	22.99	0.44	91.73	98.43	6.81
G_7	29.53	29.07	1.58	93.56	99.34	5.82
G_8	13.09	13.16	0.55	45.87	48.43	5.30

indicating that the accuracy of the model's prediction regarding the initial stage of accelerated deformation is higher than that about the pre-sliding stage, and the regular characteristics are consistent with the laws evidenced by the SSWOPP landslide.

Conclusion

(1)   Based on the study of the relation between strain and time in the accelerated creep stage of rock, this paper proposes a nonlinear viscous component based on the theory of rock creep, and through the parallel combination with the plastic component, a new nonlinear viscoplastic body can reflect the characteristics of rock's accelerated creep, and then construct the creep model of the viscoplastic body. Given that the displacement of the creep bedding rock landslide is extremely similar to the characteristics of rock creep, the creep model of nonlinear viscoplastic body is introduced into the prediction of displacement in the accelerated deformation stage of creep bedding rock landslides, and a predictive model conforming to the law governing the creep bedding rock landslides is established, which can quantitatively predict the dynamic process of landslides.

(2)   Taking the SSWOPP landslide and the Jimingsi landslide as the research cases, the newly proposed displacement prediction model is employed to analyze and predict the cumulative displacement of landslides. By comparing the measured and predicted values at the selected prediction time points in the initial stage of accelerated deformation and in the pre-sliding stage, it is found that the proposed model for predicting the displacement of creep bedding rock landslides has satisfactory accuracy and applicability, and can meet the demand of landslide displacement prediction and serve as an effective way to prevent the environmental risk posed by landslides.

(3)   It can be seen from predictions results as to the initial stage of accelerated deformation and the pre-sliding stage of the SSWOPP landslide and the Jimingsi landslide, that the average R between the predicted value and actual value in the initial stage of accelerated deformation is 0.999, RE < 2% and ARE < 5%, while in the pre-sliding stage the average R between the predicted value and the actual value is 0.997, RE < 7% and ARE < 18%, indicating that as the monitoring time is extended, and as new data is continuously introduced, the accuracy of the prediction decreases.

Table 5 Comparison of cumulative predicted displacement value and actual displacement value of the Jimingsi landslide

Monitoring points	May 1, 1991–May 31, 1991				May 1, 1991–Jun 26, 1991			
	Model parameters		R	ARE (%)	Model parameters		R	ARE (%)
	$(\tau_0 - \tau_\infty)/\eta_0$	n (10^{-2})			$(\tau_0 - \tau_\infty)/\eta_0$	n (10^{-2})		
G_1	0.316	3.989	0.999	3.063	0.226	5.793	0.999	5.205
G_4	0.855	1.409	0.999	2.232	0.491	4.006	0.996	10.256
G_6	0.451	2.861	0.999	4.876	0.250	5.229	0.995	11.940
G_7	0.554	2.966	0.999	4.807	0.403	4.006	0.997	8.298
G_8	0.214	3.702	0.999	4.610	0.193	4.091	0.999	7.248

References

Lo KY, Wai RSC, Palmer JHL, Quigley RM (1978) Time-dependent deformation of shaly rocks in southern Ontario. Can Geotech J 15(4):537–547

Xu T, Xu Q, Tang CA, Ranjith PG (2013) The evolution of rock failure with discontinuities due to shear creep. Acta Geotech 8(6):567–581

Hamouda A, El-Gharabawy S (2019) Impacts of neotectonics and salt diaper on the nile fan deposit, Eastern Mediterranean. Environ Earth Sci Res J 6(1):8–18

Li C, Cai Y (2020) Effect of soil strength degradation on slope stability. Int J Des Nat Ecodyn 15(4):483–489

Huang RQ (2007) Large-scale landslides and their sliding mechanisms in China since the 20th century. Chin J Rock Mech Eng 26(3):433–454

Saito M (1965) Forecasting the time of occurrence of a slope failure, Proceedings of the 6th international conference on soil mechanics and foundation engineering. Montre al, Que. Pergamon Press. Oxford 2:537–541

Kennedy BA (1971) The problem of excavated slopes in open-pit mines, Congress. Discussion. Salt Lake City, USA 11F. Proceed. 2 Congress, Internat. Soc. Rock Mech. Belgrad 4:551–554

Brown ET, Hoek E (1978) Trends in relationships between measured in-situ stresses and depth. Int J Rock Mech Min Sci Geomech Abstr 15(4):211–215

Li C, Tang H, Hu X, Li D, Hu B (2009) Landslide prediction based on wavelet analysis and cusp catastrophe. J Earth Sci 20(6):971–977

Xu F, Wang Y, Du J, Ye J (2011) Study of displacement prediction model of landslide based on time series analysis. Chin J Rock Mech Eng 30(4):746–751

Xue L, Qin S, Li P, Li G, Oyediran IA, Pan X (2014) New quantitative displacement criteria for slope deformation process: from the onset of the accelerating creep to brittle rupture and final failure. Eng Geol 182:79–87

Zhou C, Yin K, Cao Y, Ahmed B (2016) Application of time series analysis and PSO–SVM model in predicting the Bazimen landslide in the Three Gorges Reservoir, China. Eng Geol 204:108–120

Miao FS, Wu YP, Xie YH, Li YN (2018) Prediction of landslide displacement with step-like behavior based on multialgorithm optimization and a support vector regression model. Landslides 15(3):475–488

Li, L.W., Wu, Y.P., Miao, F.S., Xue,Y., Zhang, L.F. (2019a) Displacement interval prediction method for step-like landslides considering deformation state dynamic switching. Chin J Rock Mech Eng, 38(11), 2272-2287.

Wang NQ, Wang YF, Luo DH, Yao Y (2008) Review of landslide prediction and forecast research in China. Geol Rev 54(3):355–361

Zhang CG, Zha DH, Zhou S, Zhou HX, Jiang HD (2019a) 3D visualization of landslide based on close-range photogrammetry. Instrumentation Mesure Métrologie 18(5):479–484

Luo JH, Mi DC, Huang HF, Zhang T, Sun GH, Chen DQ (2020) Intelligent monitoring, stability evaluation, and landslide treatment of a carbonaceous mudstone and shale slope in Guangxi, China. Int J Safety Security Eng 10(3):373–379

Dong JH, Xu M, Wan SM, Xie FH, Wu QH (2018) Stability analysis of accumulation body based on monitoring results of deep displacement. Instrumentation Mesure Métrologie 17(4):563–572

An JB, Sun CF (2020) Safety assessment of the impacts of foundation pit construction in metro station on nearby buildings. Int J Safety Security Eng 10(3):423–429

Kang YG, Zhang XE (2014) An improved constitutive model for rock creep. Rock Soil Mech 35(4):1049–1055

Saccenti E, Hendriks MH, Smilde AK (2020) Corruption of the Pearson correlation coefficient by measurement error and its estimation, bias, and correction under different error models. Sci Rep 10(1):1–19

Wang Z, Zhang H, Lu T, Gulliver TA (2018) Cooperative RSS-based localization in wireless sensor networks using relative error estimation and semidefinite programming. IEEE Trans Veh Technol 68(1): 483–497

Huang X, Song J, Jin H (2020) The casualty prediction of earthquake disaster based on Extreme Learning Machine method. Nat Hazards 102:873–886

Nie L, Li Z, Zhang M, Xu L (2015) Deformation characteristics and mechanism of the landslide in West Open-Pit Mine, Fushun, China. Arab J Geosci 8(7):4457–4468

Nie L, Li Z, Lv Y, Wang H (2017) A new prediction model for rock slope failure time: a case study in West Open-Pit mine, Fushun, China. Bull Eng Geol Environ 76(3):975–988

Zhang F, Yang T, Li L, Wang Z, Xiao P (2019b) Cooperative monitoring and numerical investigation on the stability of the south slope of the Fushun west open-pit mine. Bull Eng Geol Environ 78(4):2409–2429

Huang F, Zheng NN (2019) A novel frequent pattern mining algorithm for real-time radar data stream. Traitement du Signal 36(1):23–30

Qin Z, Zhang Y, Zhang S, Zhao JW, Wang TF, Shen K (2019) Identification of microscopic damage law of rocks through digital image processing of computed tomography images. Traitement du Signal 36(4):345–352

Li Y, Shi DL, Bu FJ (2019b) Automatic recognition of rock images based on convolutional neural network and discrete cosine transform. Traitement du Signal 36(5):463–469

Liu XS, Luo WQ, Li FX, Huang L (2014) Identification index of landslide evolution stake based on association rule. Geol Sci Technol Inform 33(2):160–164

Wang LW, Xie MW, Chai XQ (2014) Research on method of displacement speed ratio for spatial evaluation of landslide deformation. Rock Soil Mech 35(2):519–528

Lv GF (1994) Formation and monitoring and forecast of Jimingsi landslide. Chin J Geol Hazard Control 5(S):376–383

He KQ, Chen WG, Zhang P (2016) Real-time monitoring of dynamic stability coefficient and displacement criterion of the creep slope. Chin J Rock Mech Eng 35(7):1377–1385